Supplementary information for:

NTA-Ni lipids affect membrane phase behavior and fluorescence of lipid-like dyes

Agustín Mangiarotti[1,2*], Maria Julia Altamirano[1,2,†], Maira Celeste Dominguez[1,2,†], Natalia Wilke[1,2*]

1-Departamento de Química Biológica Ranwel Caputto, Facultad de Ciencias Químicas, Universidad Nacional de Córdoba, X5000HUA Córdoba, Argentina.

2- Centro de Investigaciones en Química Biológica de Córdoba (CIQUIBIC, CONICET), X5000HUA Córdoba, Argentina.

* corresponding authors: amangiarotti@unc.edu.ar ; natalia.wilke@unc.edu.ar

†-These authors have contributed equally.

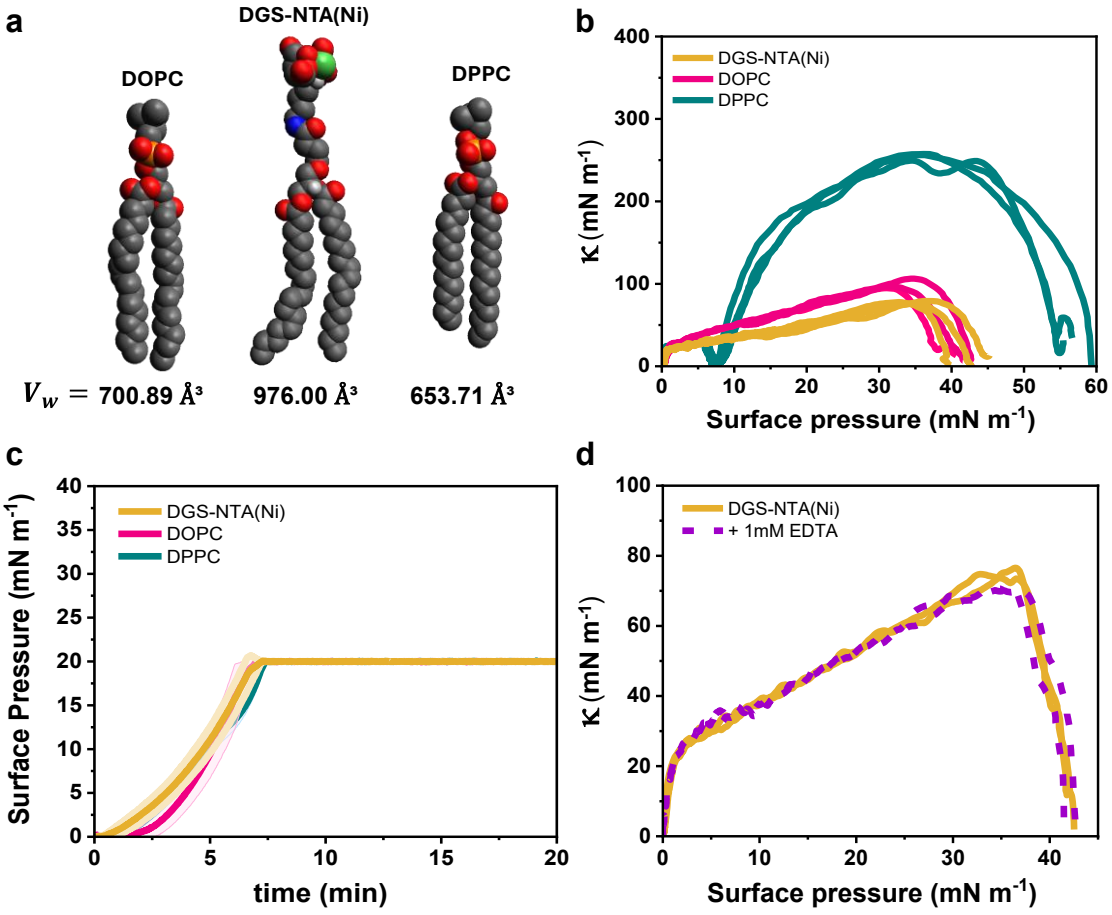

Figure S1. (a) Molecular structures of the used lipids displayed as Van der Waal spheres. The structures were generated with the open-source molecular builder and visualization tool Avogadro (v.1.2.0)[1]. The Van der Waals volume, V_w, for each structure is shown at the bottom. V_w was obtained using the free software Molovol (v1.2.0)[2] for surface computations. (b) Compressibility modulus κ *vs* surface pressure for the indicated lipids. Data for individual experiments is shown. (c) Monolayer stability measured by keeping the surface pressure constant at 20 mN m^{-1} and registering the changes in MMA, as shown in Figure 1d-e. Data shown is mean (filled lines) ±SD (shadowed area). (d) Compressibility modulus κ *vs* surface pressure for DGS-NTA(Ni) monolayers in the presence and absence of 1mM EDTA. The subphase contains 150 mM NaCl. Data for individual experiments is shown.

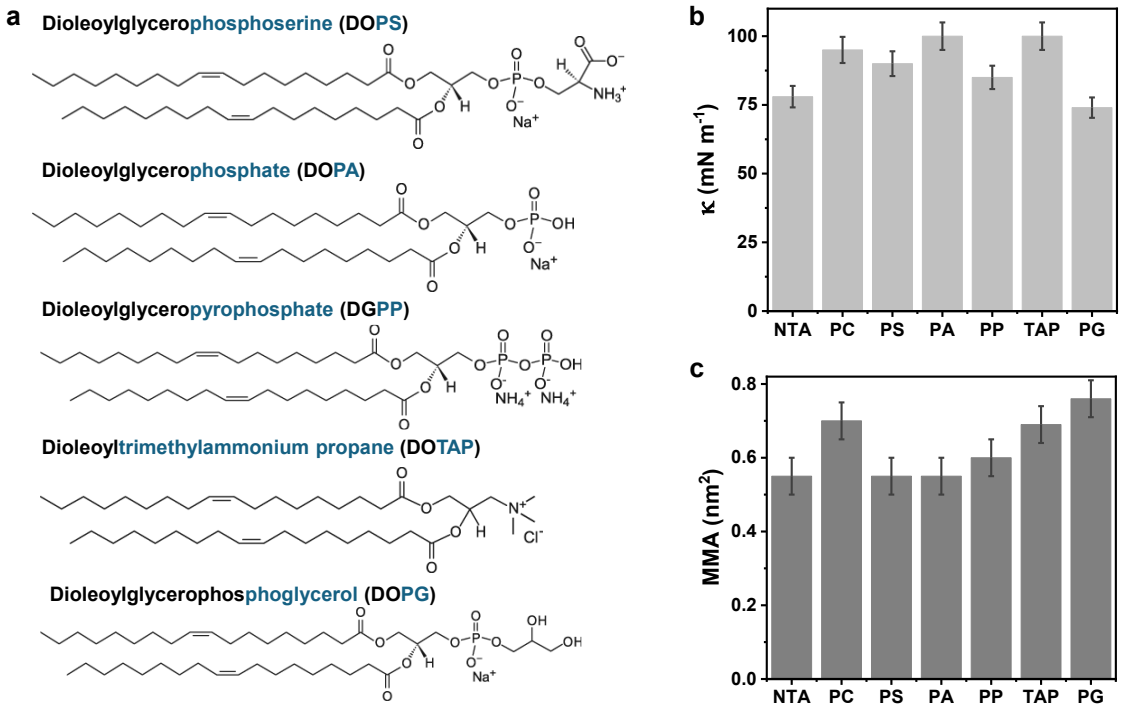

Figure S2. (a) Molecular structures of some dioleoyl lipids used for comparison. In each case the headgroup name is highlighted in blue. **(**see Fig.1 for DOPC and DGS-NTA(Ni) structures). Compressibility modulus, κ, (b) and mean molecular area, MMA (c) for the dioleoyl lipids with different headgroups. The name abbreviations correspond to those highlighted in (a) with NTA=DGS-NTA(Ni) and PC=DOPC. Mean values ± SD are shown.

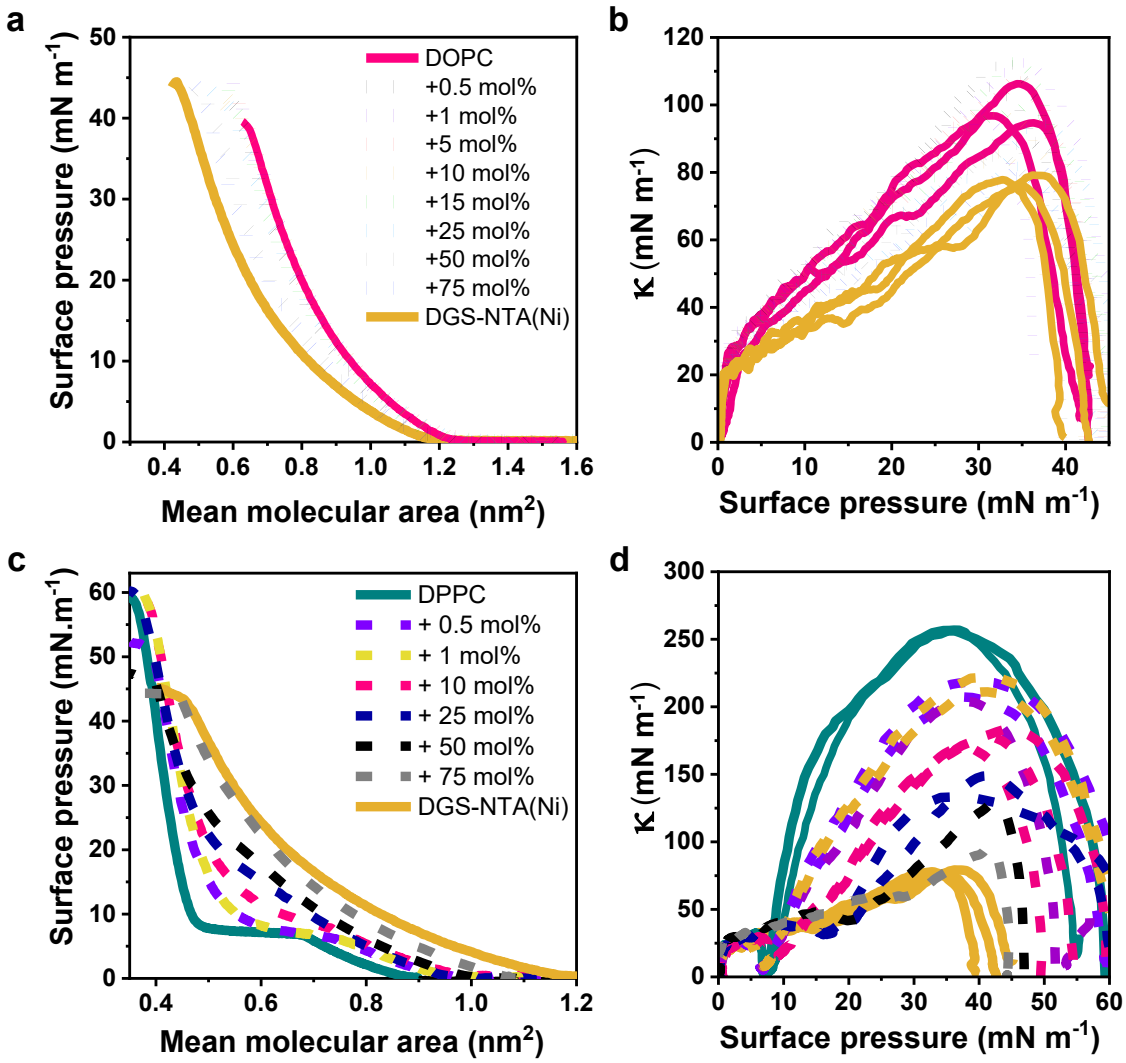

Figure S3. Langmuir monolayers and compressibility modulus for DOPC:DGS-NTA(Ni) mixtures (a-b) and DPPC: DGS-NTA(Ni) mixtures (c-d). The used compositions are indicated in the graph legends; the same color code was used for the isotherms and the compressibility modulus.

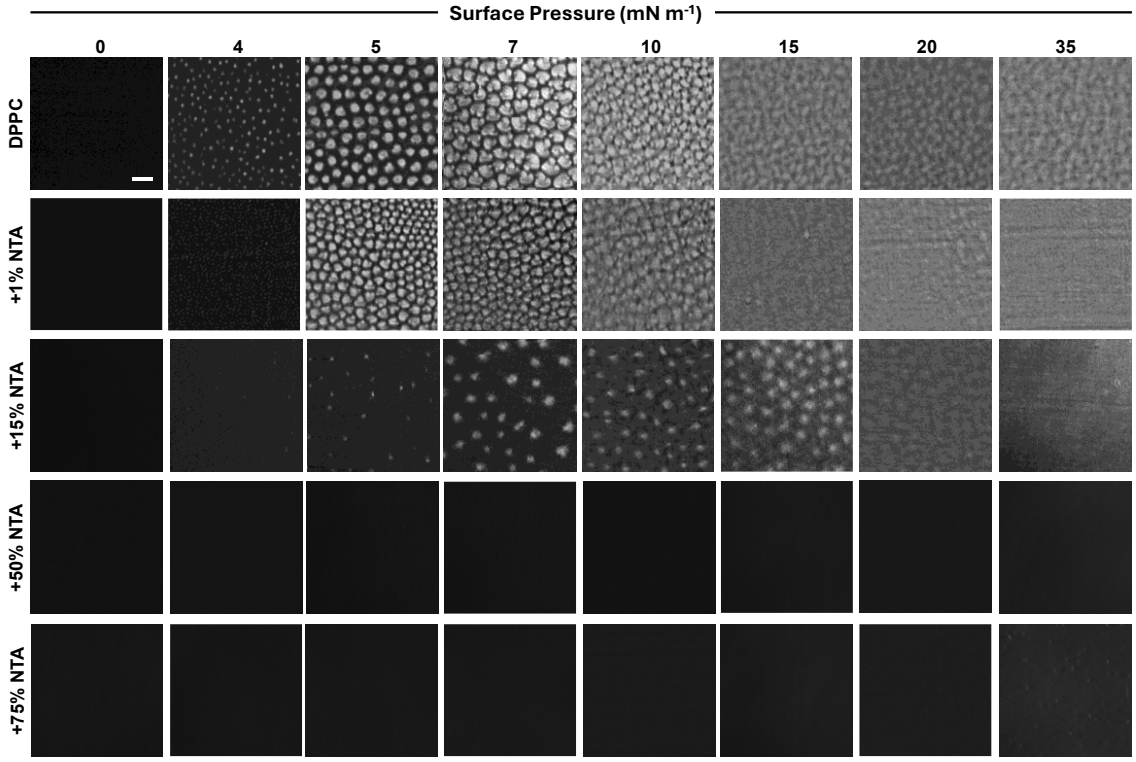

Figure S4. Brewster angle microscopy images of pure DPPC and mixtures with the indicated compositions of DGS-NTA(Ni). The phase transition is no longer visible for compositions ≥50 mol% DGS-NTA(Ni).

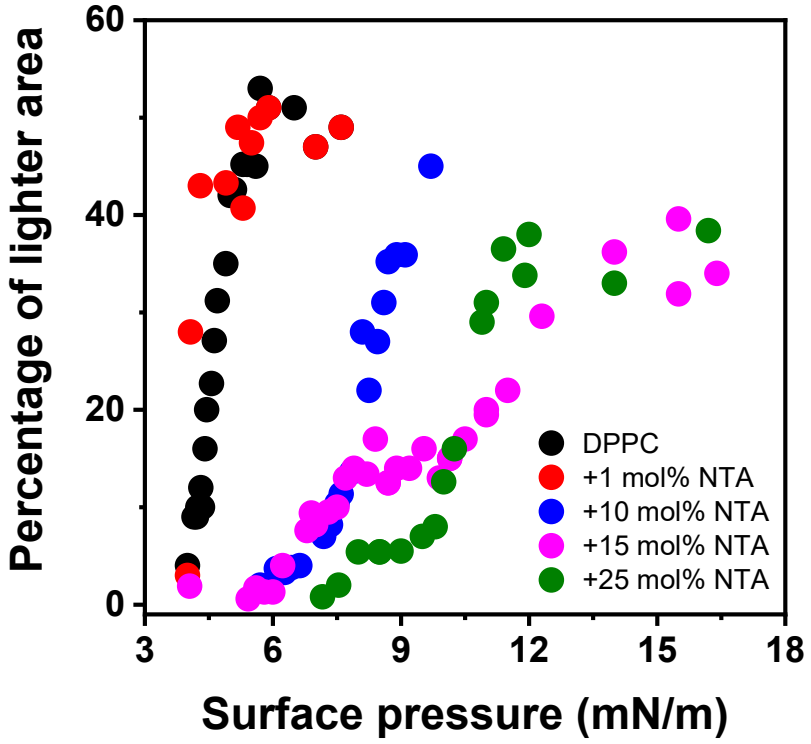

Figure S5. Percentage of the lighter area vs surface pressure taken from the BAM images. Pure DPPC and DPPC:DGS-NTA(Ni) mixtures at the indicated compositions are shown.

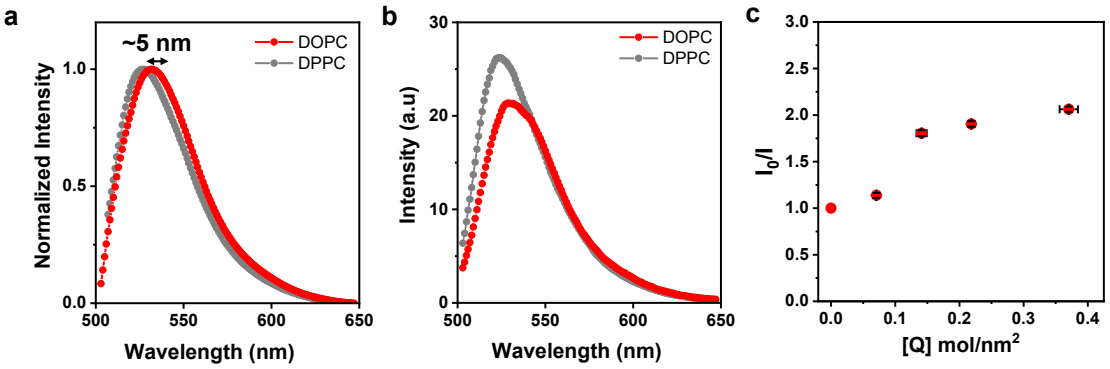

Figure S6. ATTO 488-DOPE spectrum in DOPC and DPPC MLVs: (a) The fluorescence intensity was normalized to highlight the minimal spectral shift. (b) Fluorescence intensity was not normalized to show that the increase in lipid packing produces an increase in the emitted intensity. (c) Stern-Volmer plot for ATTO488-DOPE fluorescence in the membranes shown in Figure 5a. [Q] represents the bidimensional concentration of DGS-NTA(Ni). (d) LAURDAN fluorescence spectra for DOPC and DPPC MLVs. The fluorescence intensity was normalized to highlight the high spectral shift between the two membranes.

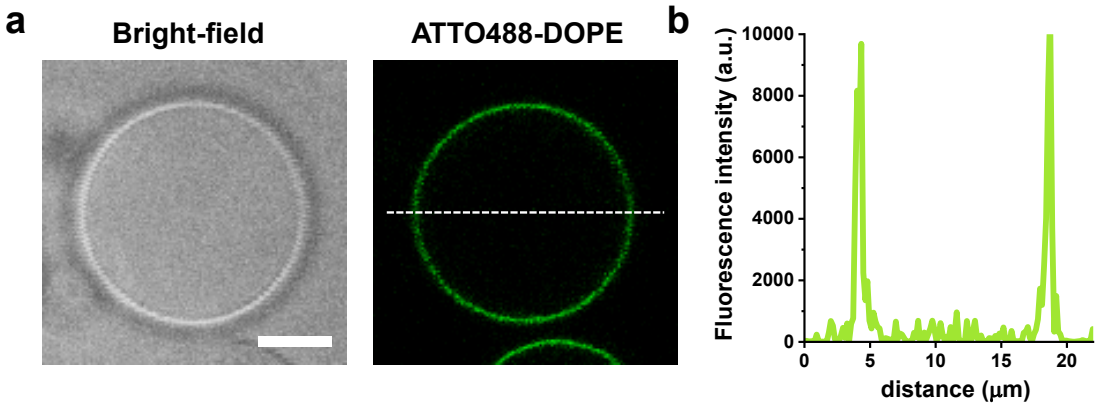

Figure S7. (a) Bright-field and confocal image of a giant unilamellar vesicle (GUV) composed of DOPC containing a 0.2 mol% ATTO 488-DOPE. Scale bar is 5 μm. (b) Intensity profile of the confocal fluorescence image shown in (a). The fluorescence intensity at the membrane is almost 10000 times higher than in the background.

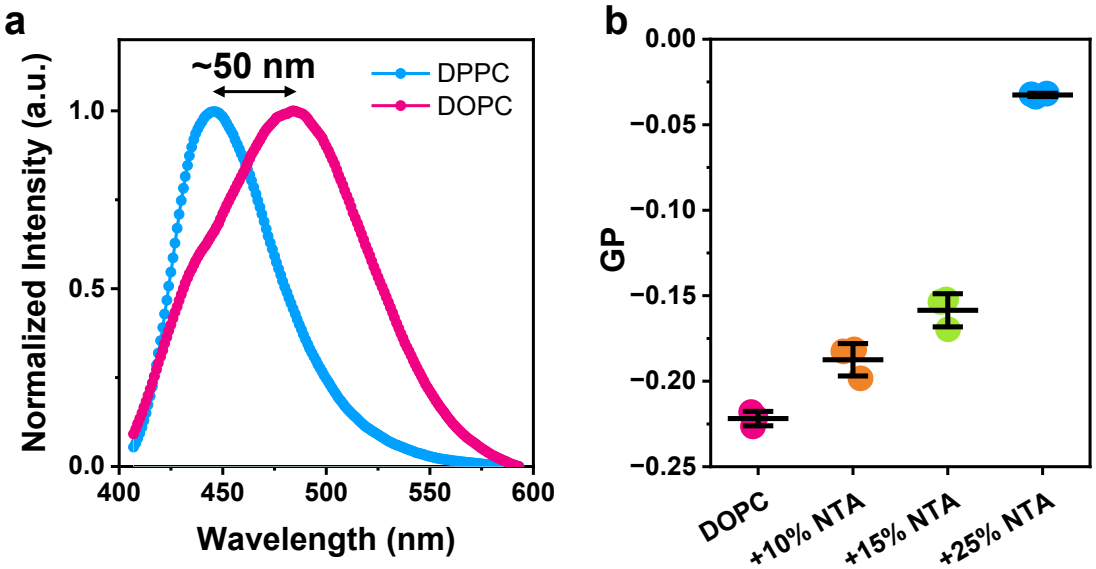

Figure S8. (a) LAURDAN fluorescence spectra for DOPC and DPPC MLVs. The fluorescence intensity was normalized to highlight the high spectral shift between the two membranes. (b) LAURDAN GP for the spectra shown in Figure 5c. $GP = \frac{I_B - I_R}{I_B + I_R}$, where I_B and I_R are the intensities at the blue and red edges of LAURDAN spectrum, respectively[3,4]. Here we used I_B= 440 nm and I_R= 490 nm.

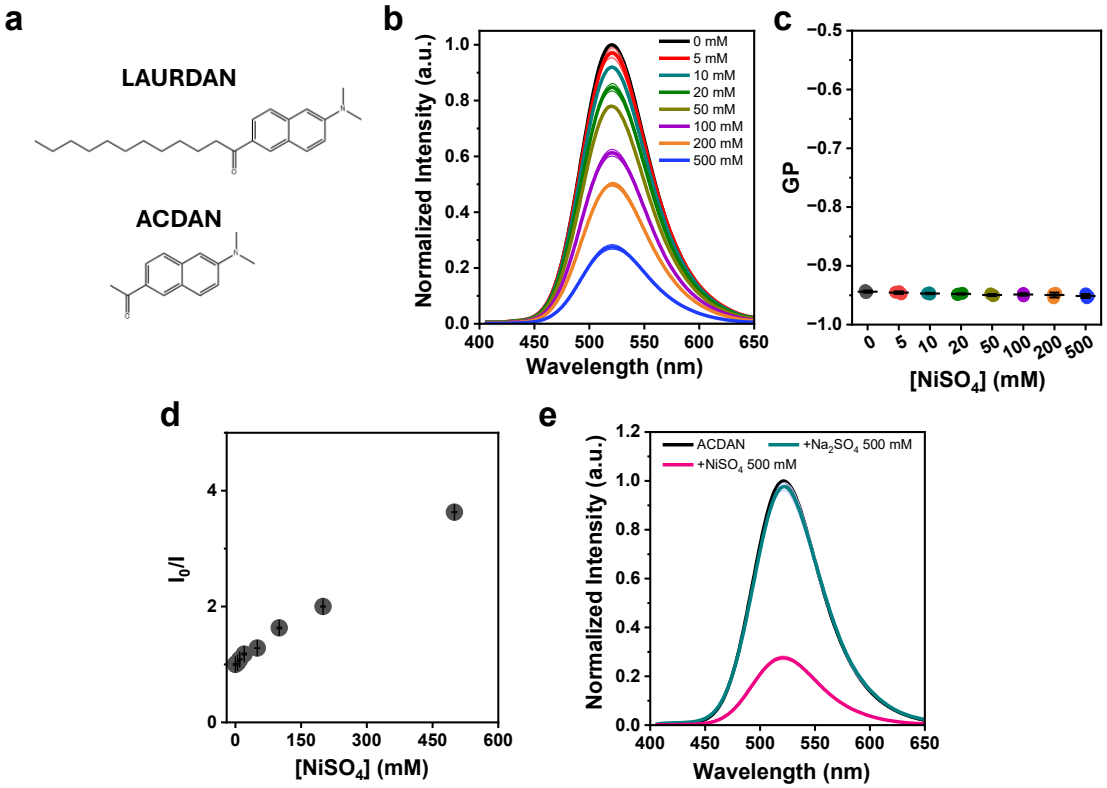

Figure S9. (a) LAURDAN (6-dodecanoyl-2-dimethylaminonaphthalene) and ACDAN (6-acetyl-2-dimethylaminonaphthalene) molecular structures. (b) Fluorescence spectra of 20 µM ACDAN solutions exposed to the indicated concentrations of nickel sulfate ($NiSO_4$). The spectra were normalized to the one of ACDAN in absence of the quencher. (c) ACDAN GP for the spectra shown in (b). As the spectral shape and maximum emission wavelength do not change, the GP values are constant for the different $NiSO_4$ concentrations. (d) Stern-Volmer plot for 20 µM ACDAN in presence of $NiSO_4$. (e) 20 µM ACDAN solution exposed to 500 mM sodium sulfate (Na_2SO_4) as a control for ionic strength effects, showing negligible effects on ACDAN fluorescence. The spectrum for $NiSO_4$ at the same concentration (500 mM) is included for comparison. For these experiments all solutions were made in buffer HEPES 10mM (pH=7.4) since nickel sulfate solutions have a very low pH when prepared in water.

References

1 Hanwell, M. D. *et al.* Avogadro: an advanced semantic chemical editor, visualization, and analysis platform. *Journal of Cheminformatics* **4**, 17 (2012). https://doi.org/10.1186/1758-2946-4-17

2 Maglic, J. B. & Lavendomme, R. MoloVol: an easy-to-use program for analyzing cavities, volumes and surface areas of chemical structures. *Journal of Applied Crystallography* **55**, 1033–1044 (2022). https://doi.org/doi:10.1107/S1600576722004988

3 Parasassi, T., De Stasio, G., Ravagnan, G., Rusch, R. M. & Gratton, E. Quantitation of lipid phases in phospholipid vesicles by the generalized polarization of Laurdan fluorescence. *Biophysical Journal* **60**, 179–189 (1991). https://doi.org/https://doi.org/10.1016/S0006-3495(91)82041-0

4 Parasassi, T., De Stasio, G., d'Ubaldo, A. & Gratton, E. Phase fluctuation in phospholipid membranes revealed by Laurdan fluorescence. *Biophysical Journal* **57**, 1179–1186 (1990). https://doi.org/https://doi.org/10.1016/S0006-3495(90)82637-0